Ilorin Journal of Science
Volume 7, Number 2, 2020, pp. 208 – 226 (Printed in Nigeria)
ISSN: 2408 – 4840 © 2020 Faculty of Physical Sciences, University of Ilorin
https://doi.org/10.54908/iljs.2020.07.02.006

ILORIN
JOURNAL OF SCEINCE

ILJS-20-002

Application of Aeromagnetic Data and Pseudogravity Transforms in the Analysis of Structures and Mineralization Potential of Osi NE, Southwestern Nigeria.

Olawuyi*, A. K.

Department of Geophysics, University of Ilorin, Nigeria

Abstract

The aeromagnetic data and pseudo-gravity transforms were used to analyze the structures and mineralization potential of Osi NE, in the Basement complex rocks of Southwestern Nigeria. The 3D Euler deconvolution was used highlight the trend characteristic of magnetic lineaments, isolate the zones where the 2 and 3D structures and their associated minerals occur in large proportions and to calculate the depth to magnetic and gravimetric basement. From the research it was deduced that; the lineament features from 3D Euler deconvolution and their mineralization which generally coincided with the river channels indicate a structural control of the drainage system and the associated mineralization in the study area, the rose plot of the extracted lineaments showed a predominance of NE-SW and NW-SE trends typical of Nigerian Basement which support Pan African as the major tectonic event while the 2 and 3D structures and their inferred mineralization show that the mineralized zones follow the geologic structures and make the study area .

Key words: Aeromagnetic data, Pseudo-gravity transforms, Structures, 3D Euler deconvolution, Mineralized Zones.

1. Introduction

The most commonly used first step in a geophysical exploration process is aeromagnetic survey permitting detection of ambient magnetic fields caused by magnetic minerals that are in the ground. Magnetic maps are often used in conjunction with other geophysical survey methods such as radiometrics, and VLF-EM to create more comprehensive geophysical and geological picture of the survey area (Gaafar, 2012; 2015). Generally, geophysical prospecting aids in the search for mineral deposits by in-situ measurements. It thus helps in target definition and delineation of ore zones (Anand *et al.*, 2001; Kwaku *et al.*, 2019). Solid mineral exploration requires interpretation of high resolution airborne data which are usually targeted at delineating possible rocks, zones and structures which can serve as host (Amigun and Anu, 2013). Integrated geophysical exploration programmes proved to be successful in identifying the sub-surface evidences of mineralization or associated structures/alteration zones (Gaafar, 2014).

*Corresponding Author: Olawuyi, A. K.
Email: gideonola2001@yahoo.com

The magnetic and gravity methods have been employed worldwide in gemstones and metalliferous mineralization target definition. These methods adopt distinct signatures that are associated with the host rock and the structural features in the mineralization target definition. The 3D Euler deconvolution has been used to calculate the depth to magnetic and gravimetric basement and to delineate the host rock and their associated mineralization using structural indices (Olawuyi *et al.,* 2016). Linear anomalies are important in the interpretation of gravity data, because they indicate some important structural features and contacts (Clotilde *et al.*, 2016). The 3D Euler Deconvolution approach of Clotilde *et al.* (2016) is quite similar to this work, but they only applied it to Bouguer data in an attempt to find depth to basement of lineaments. Olawuyi (2017) on the other hand is the proceeding of this work at the abstract level while, Olawuyi *et al.* (2016) used the same approach over Lafiagi study area but concentrated only on the 2 and 3D structures which are associated with mineral-rich rocks. Opara *et al.* (2015) in their own case uses both spectra and 3D Euler deconvolution to calculate depth to magnetic basement and to delineate the associated structural features in their chosen study area.

In this research, the aeromagnetic data and pseudo-gravity transforms have been used to analyze the structures and mineralization potential of Osi NE, Southwestern Nigeria. The 3D Euler deconvolution techniques was used to calculate the depth to magnetic and gravimetric basement and to delineate the structures and their associated mineralization using structural indices.

1.1 The Study Area

The study area covers Osi NE (Sheet 224) in the Southwestern Nigerian Basement Complex. It is bounded by latitudes $8^0$15' and $8^0$30' N and longitude $5^0$15' and $5^0$30' E, covering an area of 743 km^2 (Fig. 1). The Southwestern Nigeria is generally represented by series of older metasediments and gneisses that are known to be of Precambrian to Lower Paleozoic age (Oyawoye, 1972). The crystalline rocks of a Precambrian to probably Palaeozoic Basement Complex occupy the study area and these are represented by migmatites, banded gneiss, schist, quartzite, charnockite, amphibolite, granite gneisses and granites as discovered during the geologic field mapping exercise. Using magnetic method, Okpoli and Oludeyi (2019) described the rocks at Iwo region of southwestern Nigeria as trending approximately in the northeast-southwest direction, with most of the delineated lineaments striking mostly in

NNE-SSW, NE-SW and NW-SE with minor trend of E-W and ENE-WSW direction, in a manner suggesting that they were products of Pan African Orogeny.

The Nigerian Basement lies to the south of the Tuareg shield. Evidence from the eastern and northern margins of the West African Craton indicates that the Pan-African belt evolved by plate tectonic processes which involved the collision between the passive continental margins of the West African Craton and the active continental margin (Pharusian belt) of the Tuareg shield about 600 Ma ago (Leblanc, 1981, Caby *et al*., 1981, see also Garba, 2011). The collision at the plate margin is believed to have led to the reactivation of the internal region of the belt.

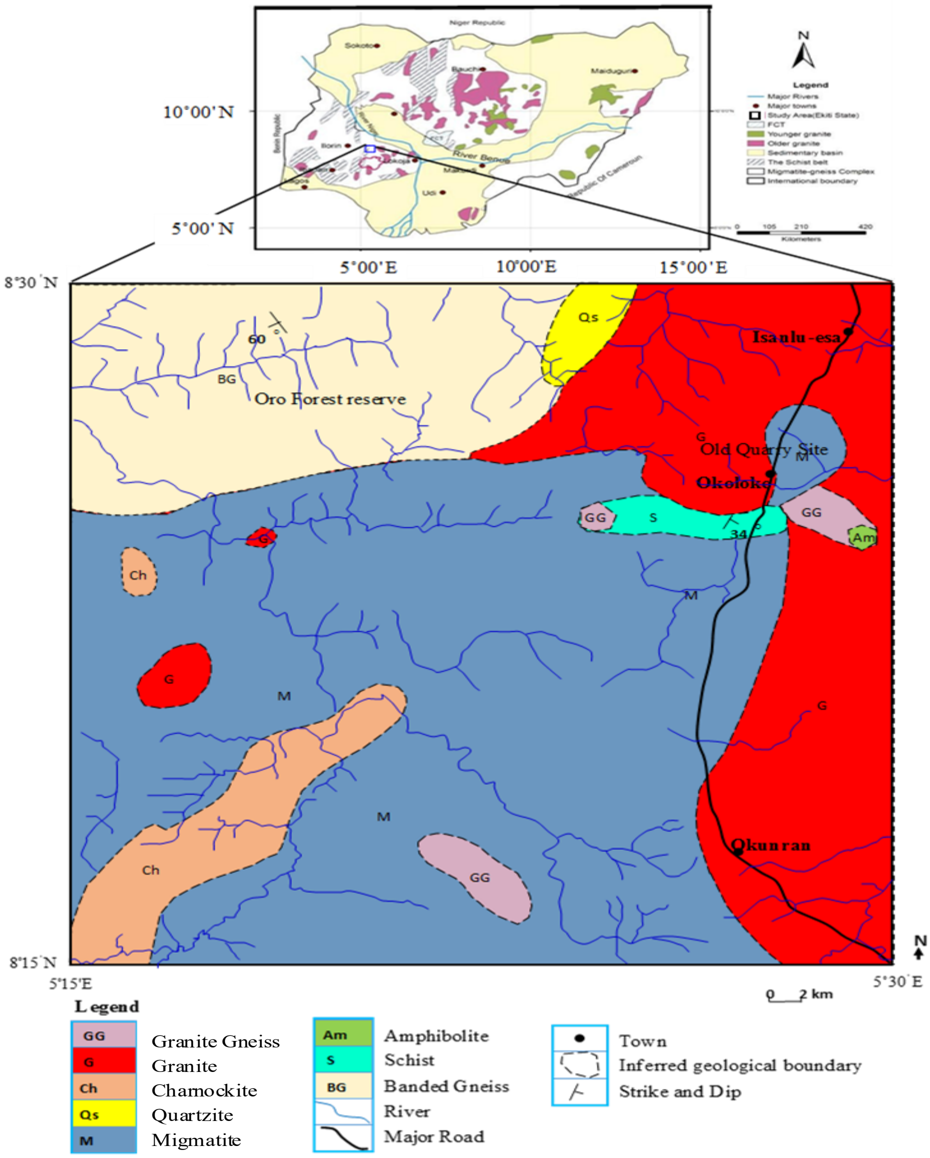

Figure 1: Geological Map of the Study Area as obtained from the field. Inset is the Geological Map of Nigeria (Adapted from Ajibade and Umeji, 1989).

The complex subsurface geology which reflects the basement tectonics could possibly be associated with faulting, folding and rifting that resulted from the reactivation/reworking that followed the Pan-African orogeny which produced the Basement Complex rocks of the study area and Nigeria (Black *et al*., 1979; Caby *et al*., 1981). The Basement Complex has been described by various authors (Oyawoye, 1972; Odeyemi, 1988) as a complex rock assemblage which includes migmatites, gneisses, quartzite, paraschists, and a series of basic to ultrabasic metamorphosed rocks which have been intruded by Pan African granites and other intrusions such as pegmatite and aplite dykes and veins, quartz veins and extrusive diorites and dolerites.

1.2 Structural Geology

Megwara and Udensi (2013) described lineaments as 'major topographic features or geologic structures that could be of regional extent usually in linear or curvilinear continuous or discontinuous over an entire length'. Ajakaiye *et al.* (1991) suggested that magnetic lineaments with definite characteristics exist within the Nigerian continental landmass. 'Some lineament patterns have been defined to be the most favourable structural conditions in control of various mineral deposits (Megwara and Udensi, 2013). Others include: 2D (i.e. vertical or horizontal cylinder or pipe) and 3D (i.e. sphere or dipole) structures.

2. Materials and Methods

2.1 Data Source and Analysis

The aeromagnetic grid map of Osi NE (Sheet 224) was procured from the Nigeria Geological Survey Agency (NGSA), Abuja, Nigeria. The data was collected at Flight Height of 80 m, Flight line spacing of 500 m, and Tie line spacing of 2000 m.

2.2 Methods

2.2.1 Regional – residual separation:

The study area does not have complex geology and it has spatial extent, thus, it seemed plausible to assume that the regional field is a first-order polynomial surface (Megwara and Udensi, 2014). The Total Magnetic Intensity (TMI) data obtained for the area was therefore stripped of a uniform value of 32,000 nT. Figure 2 is the Reduced Aeromagnetic field map of the study area. It was obtained by processing the TMI map with the Reduced - to - Equator (REDE) filter of the Oasis montaj^{TM} software. The Reduced - to - Equator (REDE) filter was used instead of the Reduction - to - Pole (RTP) to remove magnetic inclination effect since the study area is in low magnetic latitude region (Gilbert and Geldano, 1985), while the pseudogravity transforms were used to augment the magnetic data because they are easier to analyze than magnetic anomalies (Sharma, 1997) and can replicate the gravity data. It should also be noted that, for running the 3D Euler deconvolution it is not compulsory to use a reduced map, a TMI map can also be used. So it is safe to use Figure 2 above for this work.

2.2.2 The 3D Euler Deconvolution Method:

According to Davis and Li (2009), 'Euler deconvolution was originally developed in exploration geophysics for rapidly estimating the location and depth to magnetic or gravity sources. It is based on the fact that the potential field produced by many simple sources obeys Euler's homogeneity equation'. In many cases, maps of gravity and magnetic data (and transforms thereof) provide good constraints in the horizontal location of an anomaly source. Euler deconvolution adds an extra dimension to the interpretation. It estimates a set of (x,y,z) points that ideally fall inside the source of the anomaly. Euler deconvolution requires the x-,y,and z- derivatives of the data and a parameter called the Structural Index (SI) (Uieda *et al.*,2014). The location and depth determination in gridded magnetic and gravity data is normally achieved using the Euler3D menu of Oasis montaj^{TM}. The method accepts the usage of TMI grid (Uieda *et al.*, 2014), while the REDE or RTP processing is used to center the anomaly over the source. With respect to the homogeneity of the potential field, the SI varies for different fields and source types. For example, a sphere is represented by a SI of 3 and a dike is represented by a SI of 1 when dealing with total-field magnetic-anomaly data (Stravrev and Reid, 2007).

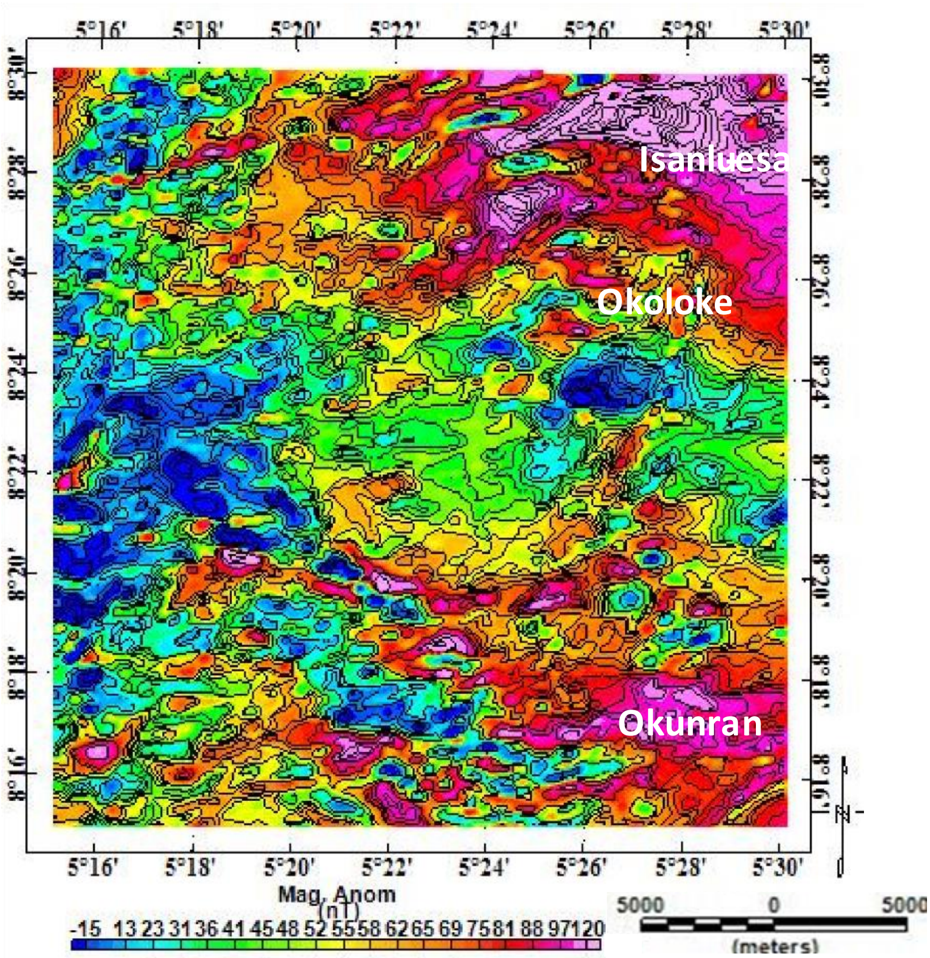

Figure 2: Superimposition of Reduced Aeromagnetic Field Map and its Contour.

Theory of Euler Deconvolution Method:

According to Davis and Li (2009), 'If a given component of the magnetic anomalous field $\Delta T(x, y, z)$ satisfies:

$$\Delta T(tx, ty, tz) = t^n \, \Delta T(x, y, z), \quad (1)$$

where n is the degree of homogeneity, then by differentiating Eq. (1) with respect to t, it can be shown that

$$x\frac{\partial \Delta T}{\partial x} + y\frac{\partial \Delta T}{\partial y} + z\frac{\partial \Delta T}{\partial z} = n\Delta T, \quad (2)$$

where x, y, and z are the coordinates of field observation points and the source is assumed to be at the origin'. Davis and Li (2009) further explained that, the degree of homogeneity is source dependent and characterizes how fast the field decreases as a function of distance to the source. As an example, they said the total-field anomaly produced by a dipolar source decreases as inverse distance cubed and the corresponding degree of homogeneity is $n = -3$; a cylinder has $n = -2$; a dyke has $n = -1$; and a contact has $n = 0$ and that typical Euler solutions for depth estimation use 0, 0.5, or 1 and since the potential field is inversely proportional to the distance raised to some power, the degree of homogeneity is non-positive and the negative of the degree of homogeneity is the structural index (SI) and will be denoted as N. In the magnetic method, structural indices range from 0 - < 0.5 (vertical geological contact) to 3 (sphere or tank) (Reynolds, 1998).

3. Result and Discussion

3.1 Pattern Interpretation of the Aeromagnetic and Pseudogravity Data

Figure 3 (a) is the Total Field Aeromagnetic Map and its contour that has been reduced to the equator using the REDE submenu of Oasis montaj^{TM} software, while Figure 3(b) is the Pseudogravity map and its contour. For qualitative analysis, the aeromagnetic and pseudogravity anomalies maps have been divided into three distinct zones and subzones of various magnetic and gravimetric characteristics based on their patterns. These include:

(i) Zone A which is characterized by anomalies with moderately high to very high magnetic reliefs (i.e. A1 and A2; Fig. 3a) with corresponding low to very low density reliefs (i.e. A1 and A2; Fig. 3b) in the Northern part of the study area. The amplitudes here vary mostly from < 52 to > 100 nT and from < -0.018 mGal to approx. 0.003 mGal for magnetic data and pseudogravity transforms respectively. The major rocks here include: banded gneiss, quartzite and granite.

(ii) Zone B which is characterized by low to intermediate magnetic reliefs (i.e. subzones B1`toB3; Fig. 3a) with corresponding high density reliefs (i.e. subzones B1 to B3; Fig. 3b) in the central part of the study area. The anomalies in this zone have amplitudes varying mostly from < -6 nT to 52 nT and 0.003 to approx. 0.025 mGal for magnetic data and pseudogravity transforms respectively. The rocks here include: migmatite, granite, schist, granite gneiss and charnockite.

(iii) Zone C is characterized by mixture of high and moderately low magnetic reliefs (i.e.subzones C1 and C2; Fig. 3a) with corresponding moderate and low pseudogravity reliefs (i.e. subzones C1 and C2; Fig. 3b). These anomalies have amplitudes of approx. 29 to > 100 nT and -0.018 to approx. 0.001 mGal for the magnetic and gravity data respectively. This zone is associated on the geological map with charnockite, granite and migmatite.

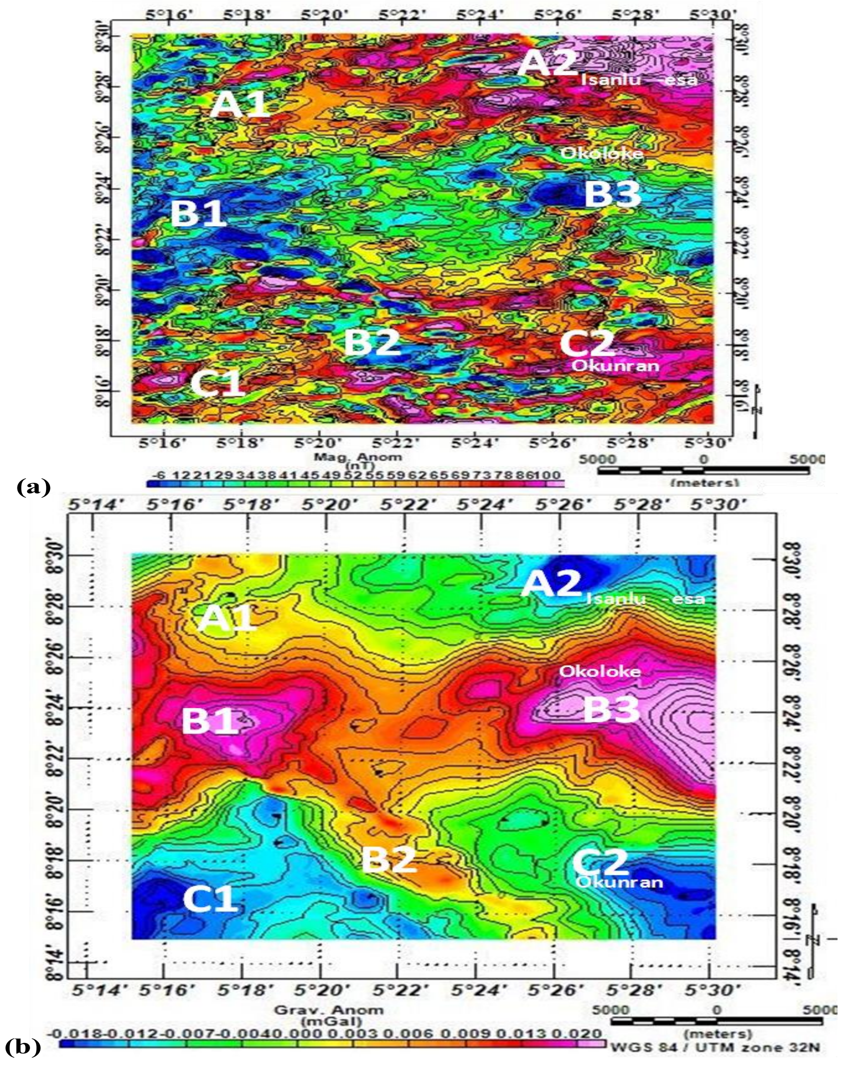

Figure 3: (a) Total Field Aeromagnetic Map (REDE) and its Contour (b) Pseudogravity Map and its Contour.

3.2 Superimposition of Zone Coloured Euler Solutions for Lineaments on Drainage Map

Figures 4 and 5 show the superimposition of zone coloured Euler solutions for near surface lineaments (i.e. magnetic S.I = 0.0 and pseudogravity S.I = 0.5 respectively) on the drainage map of the study area. The drainage in this study area has in a manner similar to the nearby Lafiagi (sheet 203) appear to be structurally controlled (Olawuyi *et al.,* 2015; 2016). This has made it possible to infer that the lineament features in this study area similarly coincide with the river channels, hence the attempt to superimpose the Euler lineaments (S.I.= 0.0 magnetic and S.I. = 0.5 pseudogravity) on the drainage map. The depth investigated is from 0 – 100m. Both maps show the predominance of the NE-SW and NW-SE trends and coincidence of the faults/lineament features or zone of discontinuities with the river channels thereby showing that the drainage in the study area is structurally controlled.

3.3 Rose Diagram

Fig. 6 is the rose plot of faults/lineament features (inferred from the structurally controlled drainage) showing the predominance of the NE-SW and NW-SE trends. This agree with the fact that the Pan African in Nigeria was followed by conjugate strike slip fault systems which average in the NE-SW and NW-SE direction and show dextral and sinistral sense of displacement that cut across the earlier Pan African structures (Wright, 1976 and Ball, 1980). Also, there is evidence of the St. Paul’s and Romanche Fracture Zones within the nearby Bida basin (Udensi *et al.,* 2003) and the bedrock at the southcentral part of the Bida basin is highly faulted: two sets of faults trending in a northwest- southeast and northeast-southwest direction (Idornighie and Olorunfemi, 1992).

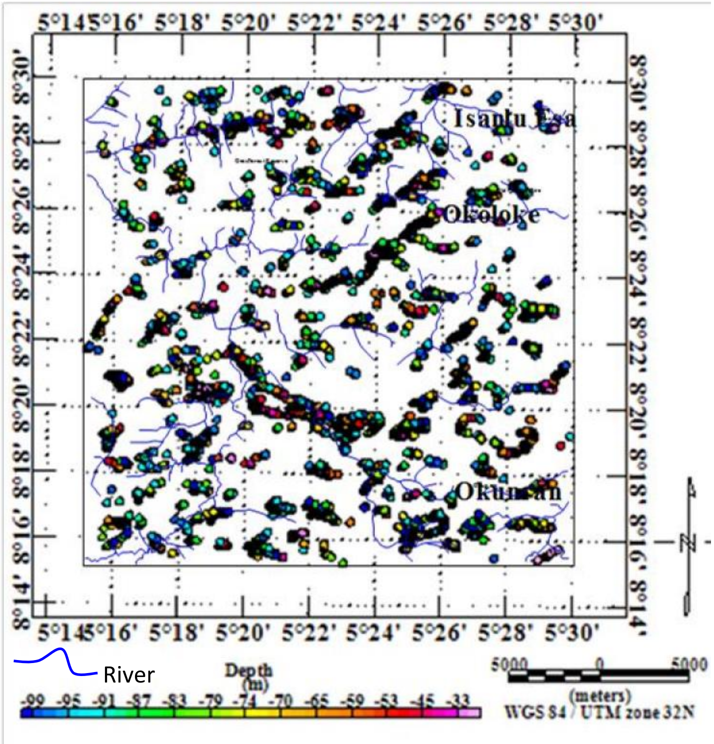

Figure 4: Superimposition of Magnetic Euler Solutions for Lineaments on Drainage Map.

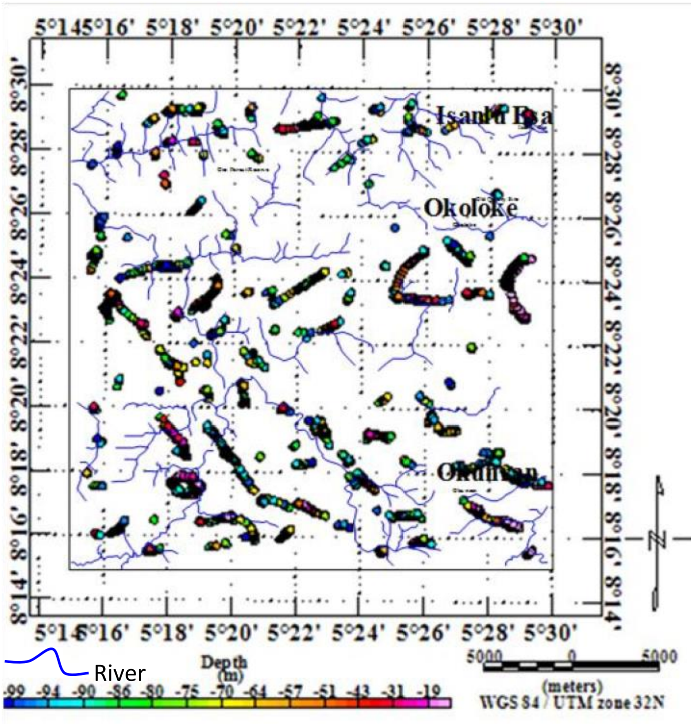

Figure 5: Superimposition of Pseudogravity Euler Solutions for Lineaments on Drainage Map.

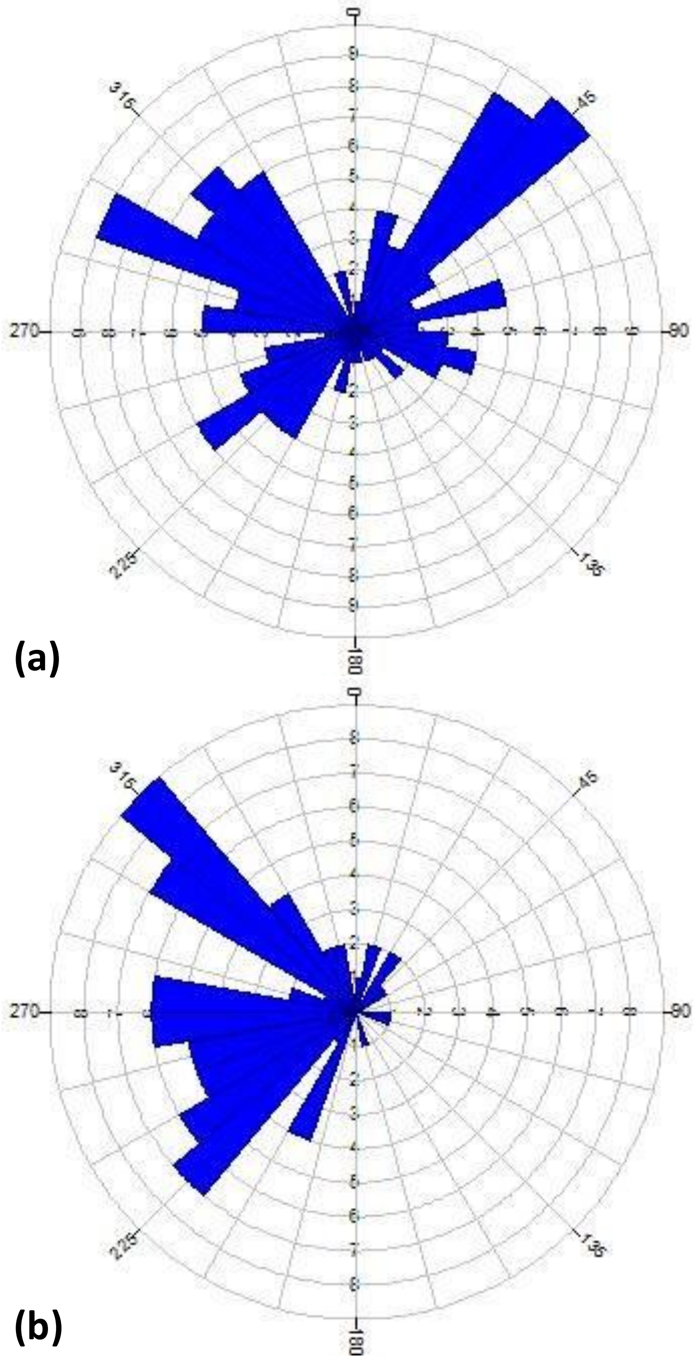

Figure 6: Rose Plot of Fault/ Lineament Features from (a) REDE lineament SI=0.5 and (b) Pseudogravity lineament SI=0.0

3.3 Zone Coloured Euler Solutions for 2 and 3-D Structures

Figures 7a and 7b show the results obtained for structural indices 2.0 (i.e. vertical or horizontal cylinder model; magnetic) and 3.0 (i.e. sphere or dipole model; magnetic) respectively. The zones where there are good number of clusters are labelled A to F for a particular structure (e.g pipe or sphere). They are regarded as prospective zones for mineral prospecting. In Oasis montaj^{TM}, window size determination is either by default (i.e. 20 x 20) or through iterations, as the correct SI for a given feature will give the tightest clustering of solutions or sharpest focus of results. Kimberlite pipe which is well known for hosting large quantity of minerals (diamonds and garnet) and rocks (peridotite and xenoliths) (Macnae, 1979; Barongo, 1983; Paterson *et al*., 1991; Macnae, 1995a; 1995b; Keating and Sailhac, 2004) has been detected or explored worldwide using structural index 2.0 (magnetic) of 3D Euler Deconvolution (Paterson *et al*., 1991; Cowan *et al*., 2000; Mahmoodi, 2016) while tanks and drums have been detected or explored worldwide with structural indices 3.0 (magnetic) of 3D Euler Deconvolution (Marchetti and Settimi, 2011). Figure 7c is the geologic map of the study area showing the different zones and the corresponding lithologies with the magnetic structures.

From Figures 7a, b and c which represents the magnetic 2 and 3D structures obtained from 3D Euler deconvolution and their corresponding rock types, it is clear that zone A (Banded Gneiss, Migmatite and Granite), B (Granite, Migmatite, Granite Gneiss, Schist and Amphibolite), C (Migmatite), D (Migmatite, Granite, Charnockite and Granite Gneiss), Migmatite, Granite Gneiss) and F(Granite) are the corresponding rock types for the different zones. Their rate of occurrences in the six zones are: Migmatite (5/6), Banded Gneiss (1/6), Quartzite (0/6), Granite Gneiss (3/6), Amphibolite (1/6) and Schist (1/6). Migmatite is the most predominant in term of the number of

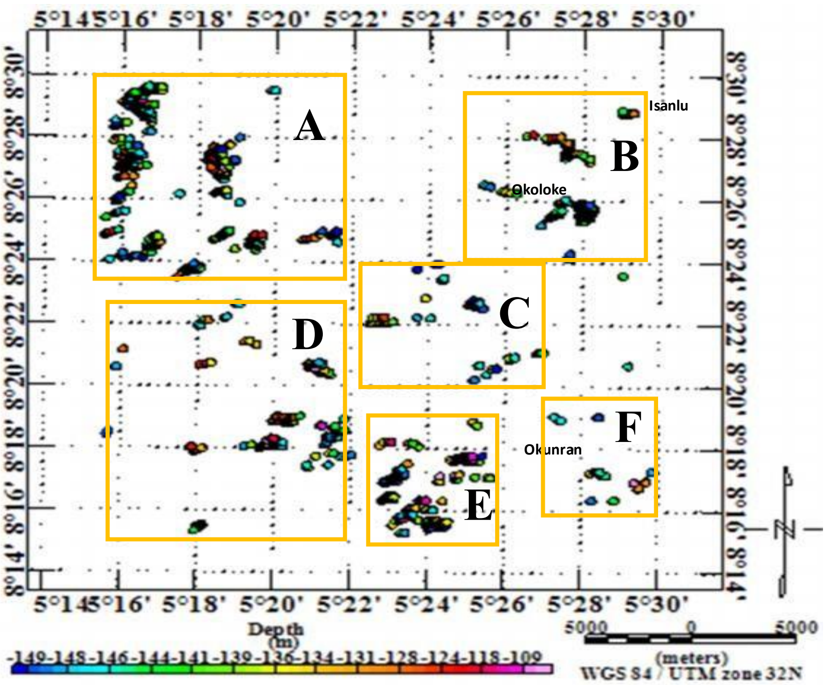

Figure 7: (a) A Typical Aeromagnetic Euler Solutions Zones Map for Pipe (S.I =2.0).

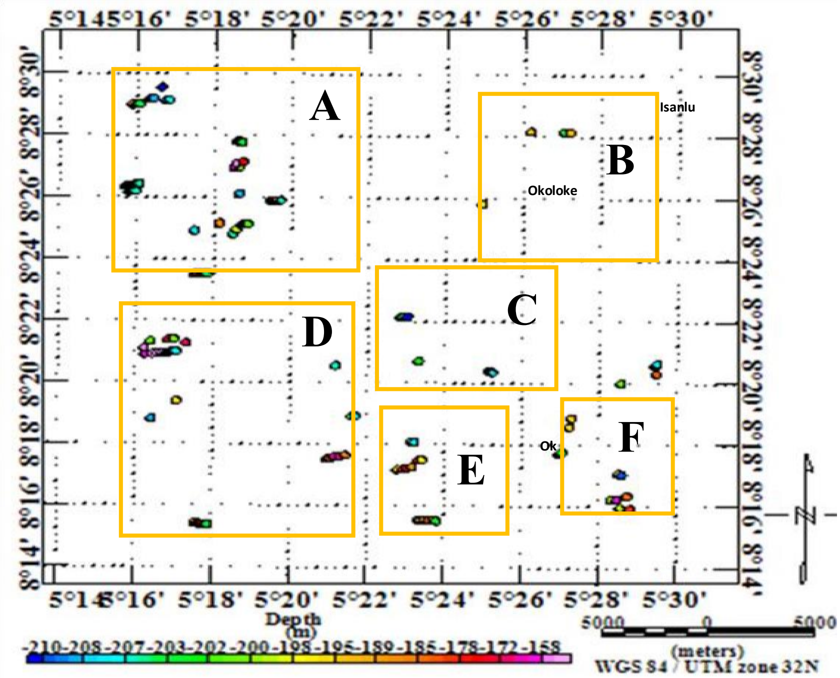

Figure 7: (b) A Typical Aeromagnetic Euler Solutions Zones Map for Sphere (S.I =3.0).

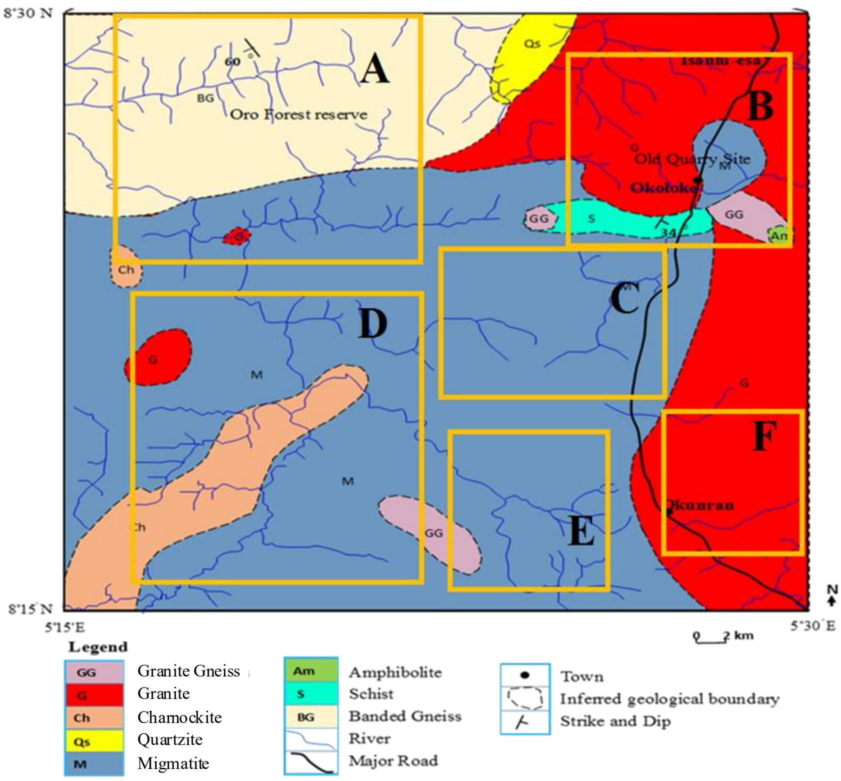

Figure 7: (c) Geological Map of the Study Area showing the Different Zones where Pipes and Spheres (Aeromagnetic) Cluster and their Corresponding Rock Types.

occurrences and the largest in size, followed by Granite. Quartzite did not appear in any of the zones A to F.

Figures 8a and 8b show the results obtained for structural indices 1.1 (i.e. pipe and dyke model; pseudogravity) and 2.0 (i.e. sphere or dipole model; pseudogravity) respectively. The areas where there are good number of clusters are labelled G to J for a particular structure (e.g pipe or sphere). Kimberlite pipe which is well known for hosting large quantity of minerals (diamonds and garnet) and rocks (peridotite and xenoliths) (Macnae, 1979; AtchutaRao and Sanker-Narayan, 1981; Barongo, 1983; Macnae, 1995a; 1996b; Keating and Sailhac, 2004) has been detected or explored worldwide using structural index 1.1 (gravity) of 3D Euler Deconvolution (Paterson *et al*., 1991, Cowan *et al.,* 2000;

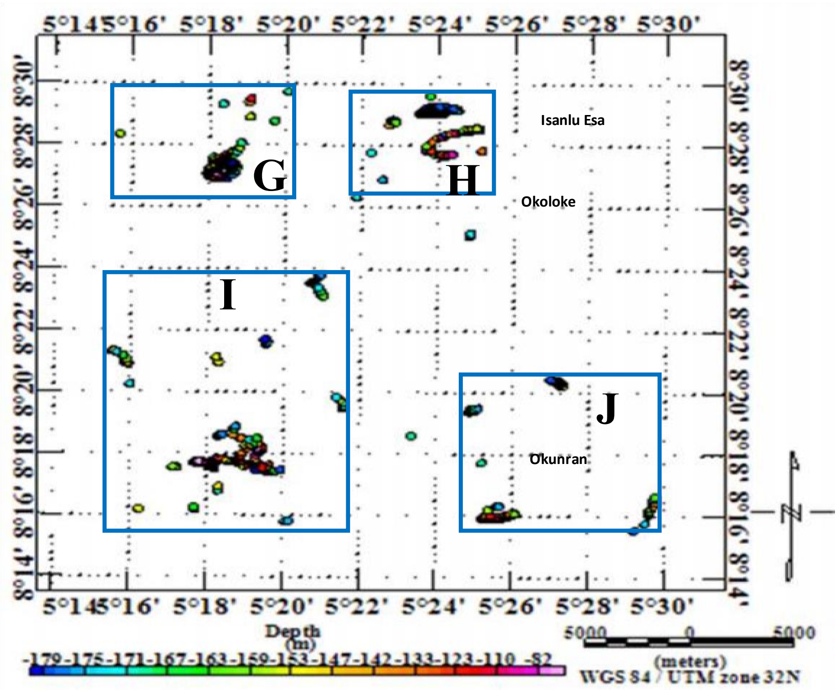

Figure 8: (a) A Typical Pseudogravity Euler Solutions Zones Map for Pipe (S.I =1.1).

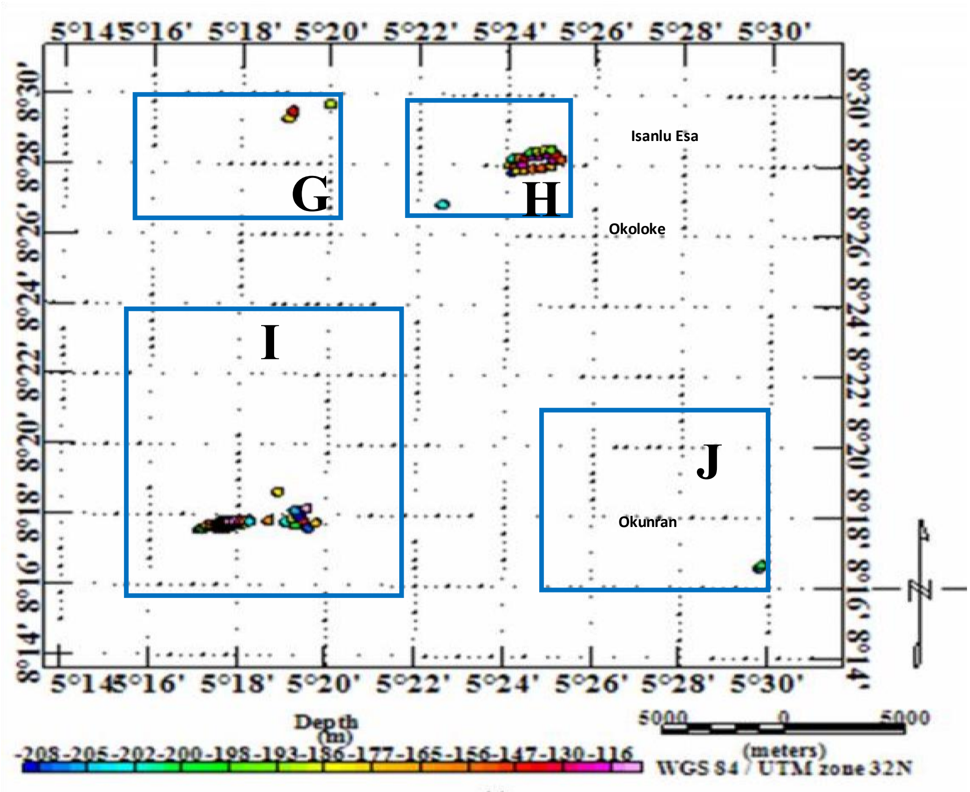

Fig. 8: (b) A Typical Pseudogravity Euler Solutions Map for Sphere (S.I =2.0 showing the Zones of Clustering.

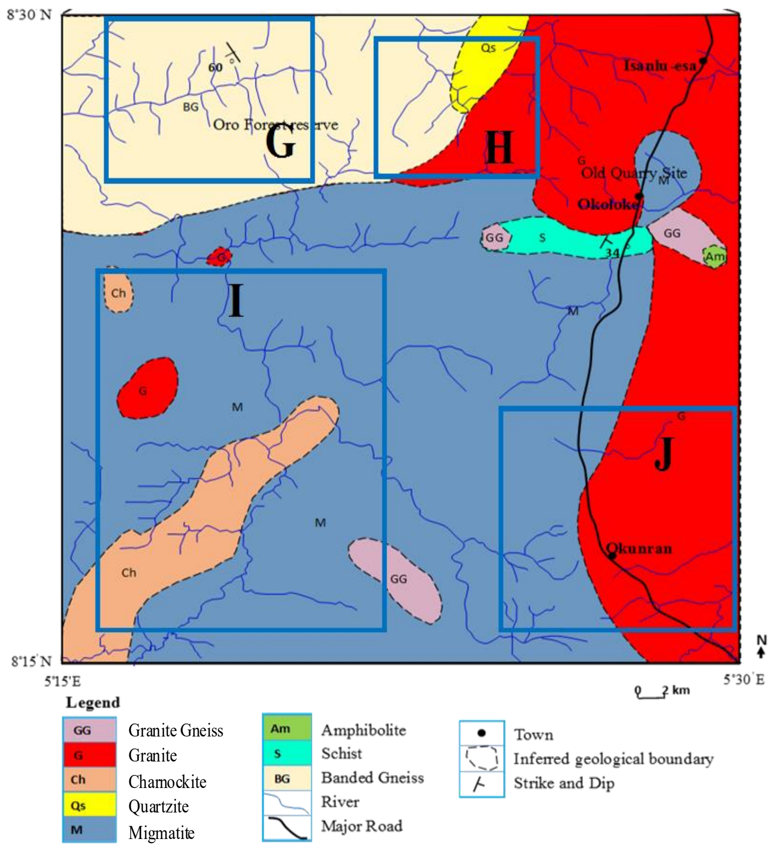

Figure 8: (c) Geological Map of the Study Area showing the Different Zones where Pipes and Spheres (Pseudogravity) Cluster and their Corresponding Rock Types.

Mahmoodi, 2016) while tanks and drums have been detected or explored worldwide with structural index 2.0 (gravity) of 3D Euler Deconvolution (Marchetti and Settimi, 2011). Figure 8c is the geologic map of the study area showing the different zones and the corresponding lithologies with the gravimetric structures.

From Figures 8a, b and c which represents the pseudogravity 2 and 3D structures obtained from 3D Euler deconvolution and their corresponding rock types, it is clear that zone G (Banded Gneiss), H (Banded Gneiss, Quartzite and Granite), I (Migmatite, Charnockite, Granite and Granite gneiss) and J (Migmatite and Granite) are the corresponding rock types for the different zones. Their rate of occurrences in the four zones are: Migmatite (2/4), Granite (3/4), Banded Gneiss (2/4) Amphibolite (1/6) and Schist (1/6). Migmatite is the largest in size but occurred in only 2 zones, followed by Granite and Banded Gneiss, both of which are almost the same in size. Others occurred in different but smaller sizes.

4. Conclusions

Regional aeromagnetic data from Osi NE study area were processed for structural mapping and elucidation of the mineralization potential of the area. The lineament features are represented by faults and fractures (Figures 4 and 5), while the 2 and 3D structures are represented by vertical or horizontal cylinder to sphere or dipole (magnetic; Figures 7a and b) and pipe and dyke to sphere (pseudogravity; Figures 8a and b) model in the study area. The mapped faults and lineament features and their associated mineralization generally coincide with the river channels on the drainage map (Figures 4 and 5), which indicate a structural control of the mineralization in the study area. These set of structures which are generally oriented in the NE-SW and NW-SE directions agree with the geology of this area. Some lineament patterns have been known to be most favourable in control of various mineral deposits.

The 2D structures are represented by Euler structural indices 2.0 (i.e. vertical or horizontal cylinder model; magnetic) and 1.1 (i.e. pipe and dyke model; pseudogravity) respectively. Kimberlite pipe which is well known for hosting large quantity of minerals (diamonds and garnet) and rocks (peridotite and xenoliths) has been detected or explored worldwide using structural indices 2.0 (magnetic) and 1.1 (gravity) of 3D Euler Deconvolution. The 3D structures are represented by Euler structural indices 3.0 (i.e. sphere or dipole model; magnetic) and 2.0 (i.e. sphere or dipole model; pseudogravity) respectively. Tanks and drums have been detected or explored worldwide with structural indices 3.0 (magnetic) and 2.0 (gravity) of 3D Euler Deconvolution. From the research, it could be inferred that the mineralized zones follow the geologic structures in the area. More so, since the study is regional, it is still a preliminary study which has to be followed up by ground truthing later.

References

Ajibade, A. C. and Umeji, A. C. (1989): Precambrian Geology of Nigeria. *Geological Survey of Nigeria*. 11-41.

Ajakaiye, D. E, Hall, D. H., Ashiekaa, J. A. and Udensi, E. E. (1991): Magnetic Anomalies in the Nigerian Continental Mass Based on Aeromagnetic Surveys. *Tectonophysics*. **192**(1), 211-230.

Amigun, J. O. and Anu, A. L. (2013): Integrated Geophysical Mapping of Structures Beneath Ijero-Aramoko Area, Southwestern Nigeria: Implications for Control of Mineralization, *Acta Geologica Sinica*. **87**, 708.

Anand, R. R., Wildman, J. E., Varga, Z. S. and Phang, C. (2001): Regolith evolution and geochemical dispersion in transported and residual regolith—bronzewing gold deposit. *Geochemistry: Exploration, Environment, Analysis*. **1**(12), 256–276.

AtchutaRao, D. and Sanker-Narayan, P.V. (1981): Structural Control of Emplacement of *Kimberlite Pipes at Panna – A Suggestion from Aeromagnetics. Geoexploration*. **19** (3), 207-228.

Ball, E. (1980): An example of very consistent brittle deformation over a wide intra-continental area: The late Pan African fracture system of the Tuareg and Nigerian shield: *Tectonophysics*. **61**, 363-379.

Barongo, J. O. (1983): Geophysical Investigations for Kimberlite Pipes in the Greenstone Belt of Western Kenya. *Journal of African Earth Sciences*. **1** (3-4), 235 - 253.

Black, R., H., Ba, E., Ball, J. M. I., Bertrand, A. M., Boullier, R., Caby, I., Davison, J., Fabre, M. L. and Wright, I. I. (1979): Outline of the Pan African geology of Andrar des Iforas (Republic of Mali): *Geologische Rundschau*. **68** (2), 543-564.

Caby, R., Bertrand, J. M. I. and Black, R. (1981): *Pan-African Ocean Closure and Continental Collision in the Horgar-Iforas Segment. Central Sahara*, In Precambrian Plate tectonics, edited by A. Kroner, Elsevier Amsterdam, 407-434.

Clotilde, O. A. M. I., Patrick, A. S., Njingti Nfor, N., Daniel, N. J., Theopile, N. M., Rokis, K. P. and Dieudonne, B. (2016): Determination of the Structural Lineaments in the Kribi-Campo Ma'an Area from a Multi-Scale Analysis of Gravity Data using the HGM and Euler 3D Deconvolution Approaches. *International Journal of Geosciences*, 7, 1122- 1143.

Cowan, D. R., Tompkins, L. A. and Cowan, S. (2000): Screening Kimberlite Magnetic Anomalies in Magnetically Active Areas. *Exploration Geophysics*. **31**(2) 66 – 72.

Davis, K. and Li, Y. (2009): *Enhancement of Depth Estimation Techniques with Amplitude Analysis*. Presented at the 2009 International Exposition and Annual SEG Meeting in Houston.

Gaafar, I. M. (2012): Geophysical Signature of the Vein-type Uranium Mineralization of

Wadi- Eishimbai, Southern Eastern Desert, Egypt. *Arabian Journal of Geosciences*. **5**, 1185-1197.

Gaafar, I. M. (2014): Geophysical Mapping, Geochemical Evidence and Mineralogy for Nuweibi Rare Metal Albite Granite, Eastern Desert, Egypt. *Open Journal of Geology*. **4**, 108-136.

Gaafar, I. M. (2015): Integration of Geophysical and Geological Data for Delineation of Mineralized zones in the Um Nagga Area, Central Eastern Desert. Egypt. *Journal of Astronomy and Geophysics.* **4**, 86 -99.

Garba, A. A. (2011): *Geology, Geochemistry and Rare-Metal Bearing Potentials of Pegmatite of Gbugbu, Lema and Bishewa areas of North Central Nigeria*. Ph.D Thesis. University of Ilorin, Nigeria. 207.

Gilbert, D. and Geldano, A. (1985): A Computer Programme to Perform Transformations of Gravimetric and Aeromagnetic Surveys. *Computers and Geosciences*. 11, 553-588.

Idornighie, A. I. and Olorunfemi, M. O. (1992): A Geoelectric Mapping of the Basement Structures of the Southcentral part of the Bida basin and its Hydro-Geological Implications. *Journal of Mining and Geology*. **28** (1), 93-103.

Keating, P. and Sailhac, P. (2004): Use of the Analytic Signal to Identify Magnetic Anomalies Due to Kimberlite Pipes. *Geophysics*. **69** (1) 180 – 190.

Takyi-Kyeremeh, K., Wemegah, D.D., Preko, K. and Menyeh, A. (2019): Integrated geophysical study of the Subika Gold Deposit in the Sefwi Belt, Ghana. *Cogent Geoscience*. **5**(1), 1585406.

Leblanc, M. (1981): *The Late Proterozoic ophiolites of Bou Azzer (Morocco) evidence for Pan-African plate tectonics*. In Precambrian Plate Tectonics, edited by Kroner, Elsevier, Amsterdam. 435-451.

Macnae, J. C. (1979): Kimberlites and Exploration Geophysics. *Geophysics*. **44** (8), 1395-1416.

Macnae, J. (1995a): Application of Geophysics for the Detection and Exploration of Kimberlites and Lamproites. *Journal of Geochemical Exploration*. **53**, 1-3.

Macnae, J. (1995b): Esoteric and Mundane Geophysics for Diamondiferous Pipe Exploration. *Exploration Geophysics*. **26** (2/3), 131 – 137.

Mahmoodi, O. (2016): *The Search for Kimberlites: Airborne Magnetic Data Processing in the Northwest Athabasca Basin*. In Summary of Investigations 2016, **2**, Saskatchewan Geological Survey, Saskatchewan Ministry of Economy, Miscellaneous Report 2016 – 4.2, Paper A-6, 14.

Marchetti, M. and Settimi, A. (2011): Integrated Geophysical Measurements on a Test Site For Detection of Buried Steel Drums. *Annals of Geophysics*. **54** (1), 105-114.

Megwara, I. U. and Udensi, E. E. (2013): Lineaments Study Using Aeromagnetic Data over Parts of Southern Bida Basin, Nigeria and the Surrounding Basement Rocks. *International Journal of Basic and Applied Sciences*. **2**(1), 115-124.

Megwara, I. U. and Udensi, E. E. (2014): Structural Analysis Using Aeromagnetic Data: Case Study of Parts of Southern Bida Basin, Nigeria and the Surrounding Basement Rocks. *Earth Science Research*. **3**(2), 27- 42.

Odeyemi, I. (1988): Lithostratigraphy and Structural Relationships of the Upper Precambrian Metasdiments in Igarra Area, Southwestern Nigeria: In: Precambrian Geology of Nigeria. Nigerian Geological Survey. 111-125.

Okpoli, C. C. and Oludeyi, D. (2019): Aeromagnetic Mapping of Iwo Region of Southwestern Nigeria for Lithostructural Delineation. *Pakistan Journal of Geology*. **3**(2), 20-30.

Olawuyi, A. K., Ako, B. D., Omosuyi, G. O. and Adelusi, A. O. (2015): Integration of Magnetic, Gravity and Geologic Data in Mapping Geologic Structures: A Case Study of a Part of Lafiagi (Sheet 203), Southwestern Nigeria: Search and Discovery. Article No. 41737. AAPG Datapages, Inc. http://www.searchanddiscovery.com/documents/2015/41737olawuyi/ndx_

Olawuyi, A. K., Ako, B. D., Omosuyi, G. O. and Adelusi, A. O. (2016): Application of 3-D Euler Deconvolution of Aeromagnetic and Pseudogravity Transforms in Mineral Exploration: A Case Study of the Pegmatite-Rich Zones of Lafiagi, Central Nigeria. *Arabian Journal of Geosciences*. **9**(16), 1-9.

Olawuyi, A. K. (2017): *3D Euler Deconvolution of Magnetic and Pseudogravity Transforms for Mapping of Structures and Mineralized Zones in Osi NE, Southwestern Nigeria*. *Proceedings* International Conference on Magnetism and Magnetic Materials: Materials Science and Nanotechnology. London, U.K.

Opara, A. I., Emberga, T. T., Oparaku, O. I., Essien, A. G., Onyewuchi, R. A., Echetama, H. N., Muze, N. E. and Onwe, R. M. (2015): Magnetic Basement Depth Re-Evaluation of Naraguta and Environs North Central Nigeria, Using 3-D Euler Deconvolution. *American Journal of Mining and Metallurgy*. **3**(2), 29-42.

Oyawoye, M. O. (1972): *The Basement Complex of Nigeria*, In: Geology of Africa. (eds) T. F. G. Dessauvaggie, and A. J. Whiteman. Univ. of Ibadan, Nigeria. 180.

Paterson, N. R., Kwan, K. C. H., and Reford, S.W. (1991): *Use of Euler Deconvolution in Recognizing Magnetic Anomalies of Pipe-like Bodies*. Extended Abstract G/M2.6, 642-645, SEG Annual Meeting, Houston.

Reynolds, J. M. (1998): *Introduction to Applied and Environmental Geophysics*. Reynolds Geosciences Ltd. John Willey (Publisher), U.K.

Sharma, P. V. (1997): *Environmental and Engineering Geophysics*. Cambridge University Press, Cambridge. 475.

Stravrev, P. and Reid, A. (2007): Degrees of Homogeneity of Potential Fields and Structural Indices of Euler Deconvolution: *Geophysics*. **72**(1), L1- L12.

Udensi, E. E., Osazuwa, I. B. and Daniyan, M. A. (2003): Trend Analysis of the Total Magnetic Field over the Nupe Basin, Nigeria. *Nigerian Journal of Physics*. **15** (1), 143 – 151.

Uieda, L., Oliveira, V. C. (Jr.) and Barbosa, V. C. F. (2014): Euler Deconvolution of Potential-Field Data: *The Leading Edge*/SEG: Geophysical Tutorial.

Wright, J. B. (1976): Fracture Systems in Nigeria and Initiation of Fracture Zones in the South Atlantic. *Tectonophysics*. **34**, 43-47.